JACC: CARDIOVASCULAR IMAGING
VOL. 7, NO. 9, 2014

ISSN 1936-878X/$36.00
PUBLISHED BY ELSEVIER INC.
http://dx.doi.org/10.1016/j.jcmg.2014.04.016

Compressed Sensing Single-Breath-Hold CMR for Fast Quantification of LV Function, Volumes, and Mass

Gabriella Vincenti, MD,* Pierre Monney, MD,* Jérôme Chaptinel, MSc,†‡ Tobias Rutz, MD,* Simone Coppo, MSc,†‡ Michael O. Zenge, PhD,§ Michaela Schmidt, RT,§ Mariappan S. Nadar, PhD,‖ Davide Piccini, MSc,†‡¶ Pascal Chèvre, RT,*# Matthias Stuber, PhD,†‡ Juerg Schwitter, MD*

ABSTRACT

OBJECTIVES The purpose of this study was to compare a novel compressed sensing (CS)-based single-breath-hold multislice magnetic resonance cine technique with the standard multi-breath-hold technique for the assessment of left ventricular (LV) volumes and function.

BACKGROUND Cardiac magnetic resonance is generally accepted as the gold standard for LV volume and function assessment. LV function is 1 of the most important cardiac parameters for diagnosis and the monitoring of treatment effects. Recently, CS techniques have emerged as a means to accelerate data acquisition.

METHODS The prototype CS cine sequence acquires 3 long-axis and 4 short-axis cine loops in 1 single breath-hold (temporal/spatial resolution: 30 ms/1.5 $\times$ 1.5 mm^2; acceleration factor 11.0) to measure left ventricular ejection fraction ($LVEF_{CS}$) as well as LV volumes and LV mass using LV model-based 4D software. For comparison, a conventional stack of multi-breath-hold cine images was acquired (temporal/spatial resolution 40 ms/1.2 $\times$ 1.6 mm^2). As a reference for the left ventricular stroke volume (LVSV), aortic flow was measured by phase-contrast acquisition.

RESULTS In 94% of the 33 participants (12 volunteers: mean age 33 $\pm$ 7 years; 21 patients: mean age 63 $\pm$ 13 years with different LV pathologies), the image quality of the CS acquisitions was excellent. $LVEF_{CS}$ and $LVEF_{standard}$ were similar (48.5 $\pm$ 15.9% vs. 49.8 $\pm$ 15.8%; $p = 0.11$; $r = 0.96$; slope 0.97; $p < 0.00001$). Agreement of $LVSV_{CS}$ with aortic flow was superior to that of $LVSV_{standard}$ (overestimation vs. aortic flow: 5.6 $\pm$ 6.5 ml vs. 16.2 $\pm$ 11.7 ml, respectively; $p = 0.012$) with less variability ($r = 0.91$; $p < 0.00001$ for the CS technique vs. $r = 0.71$; $p < 0.01$ for the standard technique). The intraobserver and interobserver agreement for all CS parameters was good (slopes 0.93 to 1.06; $r = 0.90$ to 0.99).

CONCLUSIONS The results demonstrated the feasibility of applying the CS strategy to evaluate LV function and volumes with high accuracy in patients. The single-breath-hold CS strategy has the potential to replace the multi-breath-hold standard cardiac magnetic resonance technique. (J Am Coll Cardiol Img 2014;7:882-92)

Left ventricular ejection fraction (LVEF) is one of the most important measures in cardiology and part of nearly every cardiac imaging evaluation because it is recognized as 1 of the strongest predictors of outcome (1). It is crucial for decision making (e.g., to start or stop specific drug treatments) (2), implantation of devices (3), or assessment of the effect of experimental procedures (4). Cardiac

From the *Division of Cardiology and Cardiac MR Center, University Hospital of Lausanne, Lausanne, Switzerland; †Department of Radiology, University Hospital and University of Lausanne, Lausanne, Switzerland; ‡Center for Biomedical Imaging, Lausanne, Switzerland; §MR Product Innovation and Definition, Healthcare Sector, Siemens AG, Erlangen, Germany; ‖Imaging and Computer Vision, Siemens Corporation, Corporate Technology, Princeton, New Jersey; ¶Advanced Clinical Imaging Technology, Siemens Healthcare IM BM PI, Lausanne, Switzerland; and the #Department of Radiology, University Hospital of Lausanne, Lausanne, Switzerland. There was no financial support from Siemens for this clinical study. Dr. Zenge and Ms. Schmidt are employees and stockholders in Siemens. Mr. Nadar and Mr. Piccini are employees of Siemens. All other authors have reported that they have no relationships relevant to the contents of this paper to disclose.

Manuscript received December 19, 2013; revised manuscript received April 14, 2014, accepted April 17, 2014.

magnetic resonance (CMR) is generally accepted as the gold standard to yield the most accurate measures of LVEF and left ventricular (LV) volumes and mass. These characteristics, together with the additional value of CMR to characterize pathological myocardial tissue, were the basis for CMR to be recommended for heart failure work-up in U.S. guidelines (5) and to be assigned a class I indication in the new European heart failure guidelines (6).

SEE PAGE 893

The evaluation of LV volumes and LVEF is based on well-defined and generally-accepted CMR protocols (7,8), and it involves the acquisition of a stack of LV short-axis cine images that are acquired in multiple breath-holds. Quality criteria (9) for these functional images are available and have been implemented (e.g., within the European CMR registry) (10). Although standard protocols are well established, it is desirable to speed up CMR acquisitions to reduce motion artifacts in severely ill patients who cannot hold their breath for an extended amount of time, to increase spatial and/or temporal resolution per unit time of acquisition, or simply to shorten the CMR examination. A variety of recent acceleration techniques (11), such as spatiotemporal correlations (12–14) and spatially selective excitations (15), could speed up acquisitions several fold. As an alternative, compressed sensing (CS) was recently proposed as a means to considerably accelerate data acquisition. Conventional magnetic resonance (MR) images once acquired can be compressed with little or no perceptible loss of information (e.g., by JPEG standards). The concept of CS aims to no longer apply such compression algorithms to the acquired magnetic resonance image data but to the acquisition process itself and then to reconstruct the undersampled data with novel nonlinear reconstruction algorithms (Online Appendix) (16). This helps accelerate image acquisition several fold and theoretically enables a cine acquisition of the whole heart in 1 single breath-hold, whereas conventional data acquisition that covers the whole heart by short axes often lasts up to 10 min. The aim of the study was to demonstrate that this CS concept: 1) is applicable to the heart in a clinical setting; 2) produces data to accurately quantify LV function, volumes, and mass; and 3) provides data quality that allows for acceptable measurement reproducibility.

METHODS

CS TECHNIQUE. The prototype CS sequence developed for this study achieves incoherent sampling by initially distributing the readouts pseudo-randomly in the Cartesian k-space (17). In addition, for cine-CMR, a pseudo-random offset is applied from frame to frame that results in temporal incoherence. Finally, a variable sampling density in k-space stabilizes the iterative reconstruction. The reconstruction program is implemented directly on the scanner and runs a nonlinear iterative reconstruction (80 iterations) with k-t regularization derived from a parallel imaging reconstruction that takes coil sensitivity maps into account. For cine CMR, no additional reference scans are needed because the coil sensitivity maps are intrinsically calculated from the temporal average of the input data in a central region of k-space (**Table 1**, Online Appendix).

ABBREVIATIONS AND ACRONYMS

CMR = cardiac magnetic resonance

CS = compressed sensing (technique)

LVEDV = left ventricular end-diastolic volume

LVEF = left ventricular ejection fraction

LVESV = left ventricular end-systolic volume

LVSV = left ventricular stroke volume

STUDY PROTOCOL. Healthy volunteers (n = 12) and patients with different pathologies of the LV (n = 21) were included in the study. The robustness and precision of the CS approach to measure LVEF and LV volumes and mass were assessed in comparison with a standard high-resolution steady-state free precession cine CMR approach. All CMR examinations were performed on a 1.5-T magnetic resonance scanner (MAGNETOM Aera, Siemens AG, Erlangen, Germany). The imaging protocol consisted of cardiac localizers followed by the acquisition of a stack of conventional short-axis steady-state free precession cine images covering the entire LV (**Table 1**). Next, to test the new CS-based technique, slice orientations

TABLE 1 Imaging Parameters of the Standard Cine Sequence (Standard SSFP), Prototype CS-Based Cine Sequence, and Phase-Contrast Flow Sequence (Aortic Flow)

	Standard SSFP	CS Technique	Aortic Flow
TR, ms	3.06	2.94	10.5
TE, ms	1.28	1.23	3.04
Field of view, mm	300 × 240	420 × 340	340 × 238
Image matrix	256 × 180	272 × 272	192 × 192
Spatial resolution, mm	1.2 × 1.2	1.5 × 1.5	1.8 × 1.8
Temporal resolution, ms	49	30	42
Slice thickness/gap, mm	8/2	6	6
Flip angle	60°	70°	20°
Bandwidth, Hz/pixel	930	875	491
k lines/segment	16	10	4
Cardiac phases	25*	24†	20*
Breath-holds, n (duration of breathhold, s)	4–6 (12)‡	1 (14)§	1 (20)
VENC, cm/s	–	–	150

*Retrospective electrocardiogram (ECG) triggering. †Prospective ECG triggering. ‡To cover the LV in this study population, 4 to 6 breath-holds (i.e., 8 to 12 short-axis slices) were required. §Seven slices were acquired in 1 breath-hold to cover the LV.

CS = compressed sensing; LV = left ventricle; SSFP = steady-state free precession; TE = echo time; TR = repetition time; VENC = velocity encoded.

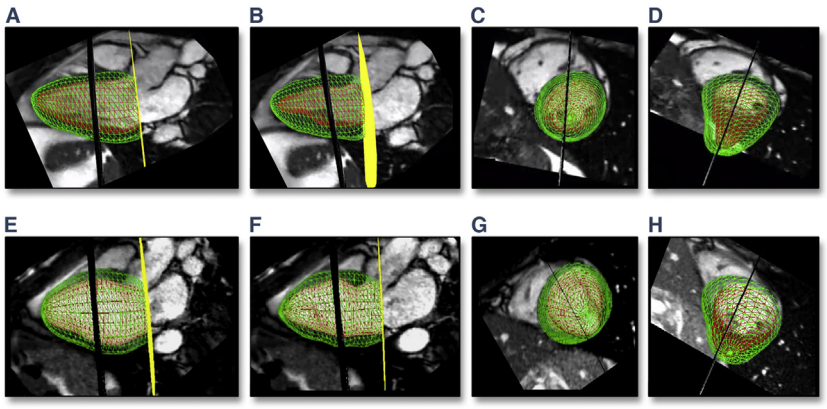

FIGURE 1 3D Reconstruction Derived From 7 Slices Acquired Within a Single Breath-Hold

The tracking of systolic left ventricular (LV) long-axis shortening allows for accurate LV volume measurements (**yellow plane** indicates mitral valve plane) in a volunteer **(A to D)** and in a patient with ejection fraction of 32% **(E to H)**. Any orientation of the 3-dimensional (3D) representation of the LV is available for inspection of function.

TABLE 2 Characteristics of Study Population (N = 33)

	Volunteers (n = 12)	Patients (n = 21)	p Value
Age, yrs	33 ± 8	63 ± 14	<0.0001
Male	9 (75)	18 (86)	–
BMI, kg/m^2	25.2 ± 5.1	26.2 ± 3.6	0.527
BSA, m^2	1.9 ± 0.2	1.9 ± 0.19	0.394
Rhythm, SR/PVCs/PM	12/–/–	19/1/1	–
HR, beats/min	66 ± 10	71 ± 13	0.203
Cardiovascular risk factors	–	18 (85)	–
Family history of CAD	–	3 (14)	–
Hypertension	–	11 (52)	–
Hypercholesterolemia	–	13 (62)	–
Diabetes	–	3 (14)	–
Smoking	–	10 (47)	–
Diagnosis			
Coronary artery disease*	–	14 (66)	–
Valve pathology†	–	16 (76)	–
Moderate to severe	–	6 (28)	–
Minimal to mild	–	9 (43)	–
Ross procedure	–	1 (5)	–
Cardiomyopathy	–	3 (14)	–
AV block (CMR-conditional PM implanted)	–	1 (5)	–
Congenital heart disease‡	–	1 (5)	–
LV measurements			
LVEF, %	60.9 ± 15.4	41.4 ± 15.4	0.0002
LVEDV, ml	151.8 ± 25.1	175.0 ± 70.9	0.284
LVESV, ml	59.9 ± 15.5	111.1 ± 77.0	0.031
LVSV, ml	91.9 ± 14.1	63.9 ± 20.4	0.0002
LV mass, g	123.7 ± 30.7	135.6 ± 33.7	0.323

Values are mean ± SD or n (%). *Patients with coronary artery disease underwent adenosine stress testing and/or assessment of viability. †No echocardiography available in 2 patients. ‡Follow-up CMR examination after a Ross procedure for congenital aortic valve stenosis.

AV = atrioventricular; BMI = body mass index; BSA = body surface area; CAD = coronary artery disease; CMR = cardiac magnetic resonance; HR = heart rate; LV = left ventricular; LVEDV = left ventricular end-diastolic volume; LVEF = left ventricular ejection fraction; LVESV = left ventricular end-systolic volume; LVSV = left ventricular stroke volume; PM = pacemaker; PVC = premature ventricular contraction; SR = sinus rhythm.

were planned to cover the LV with 4 short-axis slices (positioned at roughly equidistant positions along the LV long axis) complemented by 3 long-axis slices (i.e., 2-, 3-, and 4-chamber slices). The long-axis acquisitions were added to benefit from the high in-plane spatial resolution to follow the mitral annulus motion during the cardiac cycle. Because the reconstruction algorithm is susceptible to aliasing in the phase-encoding direction, the 7 slices were first acquired with a non-cine acquisition to check for correct phase-encoding directions and, if needed, to adjust the field-of-view to avoid fold-over artifacts. After confirmation of correct imaging parameters, the multislice prospectively electrocardiogram-triggered CS acquisition was performed in a single breath-hold (14 heart beats; acceleration factor 11.0) (Table 1). As a reference, a phase-contrast flow measurement (Table 1) in the ascending aorta was performed to be compared with the left ventricular stroke volumes (LVSVs) calculated from the standard and CS cine data ($LVSV_{cs}$ and $LVSV_{standard}$).

The study protocol was approved by the ethics committees of our institution, and all study participants gave written informed consent before enrollment.

IMAGE ANALYSES. The image quality of the CS and standard cine CMR images was assessed based on recently published criteria (9). Briefly, 1 point was given if an artifact (wrap around, respiratory ghost, cardiac ghost, image blurring/mistriggering, metallic, or shimming) impeded the visualization of more than one-third of the LV endocardial border at end-systole and/or diastole on a single short-axis slice. If such

TABLE 3 Image Quality

	Standard (12 Volunteers/21 Patients)				CS (12 Volunteers/21 Patients)			
	Score 0	Score 1	Score 2	Score 3	Score 0	Score 1	Score 2	Score 3
LV coverage	12/21	–	–	–	12/21	–	–	–
Wrap around	12/21	–	–	–	9/18	–/4	–	1/2
Ghosts	12/18	–/3	–	–	11/20	–	–	1/–
Image blurring/mistriggering	11/18	1/2	–/1	–	12/21	–	–	–
Metallic artifact	12/21	–	–	–	12/21	–	–	–
Shimming artifact	12/21	–	–	–	12/21	–	–	–
Signal loss	12/21	–	–	–	12/21	–	–	–
Orientation of stack	12/21	–	–	–	12/21	–	–	–
Correct LV long axes	12/21	–	–	–	12/21	–	–	–
Slice thickness/gap	12/21	–	–	–		not applicable		
Total score	0.24 ± 0.50			0.40 ± 1.00				

Quality score for standard versus CS was not significantly different ($p = 0.36$ by Wilcoxon signed rank test).
Abbreviations as in Table 1.

artifact involved 2 or ≥3 slices, 2 or 3 points were given, respectively. For the standard cine CMR images, these criteria were applied to the short-axis acquisitions only because they are used exclusively for volume calculations. For the CS quality assessment, these criteria were applied to both the short- and long-axis CS acquisitions because these slice orientations were used for volume calculations with this approach. For quantitative measurements, the conventional stack of short-axis cine MR images was analyzed by the Argus VF software (Siemens AG) applying the Simpson rule. The CS cine data were analyzed by the 4-dimensional (4D)-VF Argus software (Siemens AG) (18). This software is based on an LV model, and with relatively few operator interactions, the contours for the LV endocardium and epicardium are generated by the analysis tool. This 4D analysis tool automatically tracks the 3-dimensional (3D) motion of the mitral annulus throughout the cardiac cycle (**Figure 1**) and thus allows for an accurate volume calculation, particularly at the base of the heart.

Aortic flow was quantified by manually tracing a region of interest on the ascending aorta of the phase-contrast CMR images corrected for any phase offset measured on the chest wall (Argus flow analysis package, Siemens AG). Because aortic flow was performed distal to the coronary arteries, flow in the coronary arteries was estimated as the LV mass multiplied by 0.8 ml/min/g divided by heart rate (19). This flow was added to the aortic flow before comparison versus volumetrically-determined LVSV. Patients were excluded from this analysis because the presence of a mitral regurgitation of any degree would cause an overestimation of the volumetric LVSV in the patient group.

To assess intraobserver and interobserver reproducibility of the CS technique, the CS cine images were analyzed by 2 experienced cardiologists (G.V. and P.M. [CMR level III experts]).

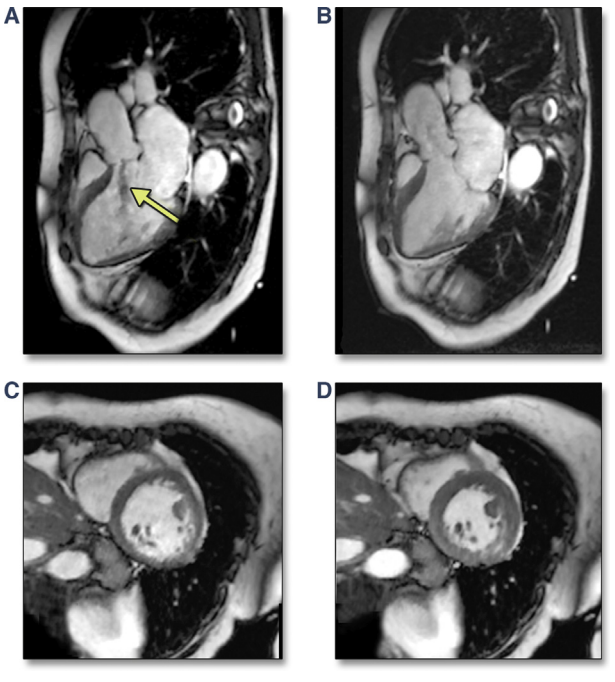

FIGURE 2 Good-Quality Compressed Sensing Acquisition in a 79-Year-Old Patient

Quality score was 0 in a 79-year-old patient with left ventricular systolic dysfunction (left ventricular ejection fraction 41%) and severe aortic regurgitation **(arrow)** before aortic valve replacement. No flow-related or fold-over artifacts are visible. **(A and B)** Three-chamber view in diastole/systole. **(C and D)** Short-axis view in diastole/systole. Abbreviation as in Figure 1.

STATISTICAL ANALYSES. The standard multi-breath-hold and the novel single-breath-hold CS techniques were compared using Bland-Altman (20) and linear regression analyses. The same analyses were performed to assess interobserver and intraobserver variabilities of the CS technique. Comparisons of demographic and CMR data (Table 2) involved the unpaired 2-tailed Student *t* test. Differences in quality scores between the standard multi-breath-hold and CS technique were explored using the nonparametric Wilcoxon matched-pairs signed-rank test. Differences between LVSV and aortic flow were evaluated by paired Student *t* test. Values of $p < 0.05$ were considered statistically significant. Stata 12 software (StataCorp LP, College Station, Texas) was used for statistical analyses.

RESULTS

STUDY POPULATION AND IMAGE QUALITY. Demographic data and image quality scores are given in Tables 2 and 3, respectively. Excellent image quality of the single-breath-hold multislice CS acquisitions was obtained with a mean score of 0.39 ± 0.79 (not different from that of standard CMR: 0.24 ± 0.50; p = 0.36) (Table 3, Figures 2, 3, and 4). Two CS acquisitions had poor image quality (score ≥3) due to fold-over artifacts (Figures 5A and 5B). Nevertheless, all CS data were of adequate quality for quantitative 4D analysis (Figure 1). Figures 5C and 5D show examples of flow-related artifacts. Although small structures such as trabeculations were visualized in the CS data, smaller anatomic details such as branches of coronary arteries were not detectable on the CS images.

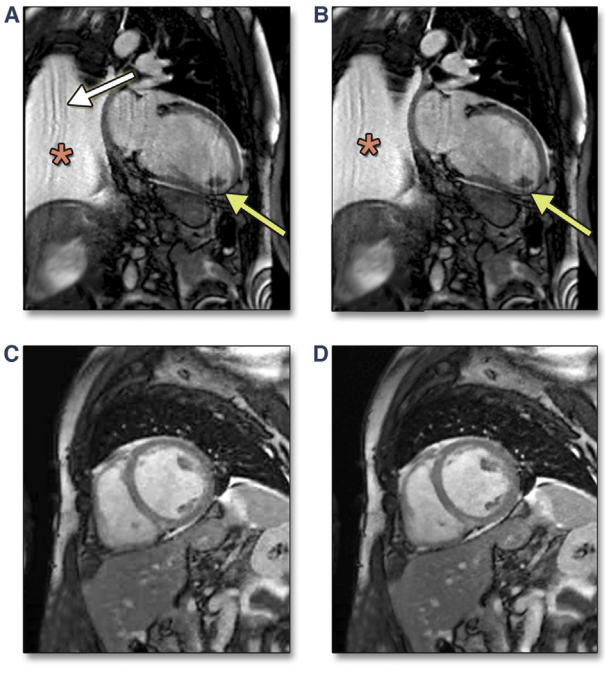

FIGURE 3 Compressed Sensing Acquisition in a 58-Year-Old Patient With Dilated Cardiomyopathy

Patient had a left ventricular ejection fraction of 8%, an apical thrombus **(yellow arrow)**, and pleural effusion **(asterisk)**. Mild fold-over artifact in the 2-chamber view **(white arrow)**; quality is sufficient to detect the apical thrombus (quality score of 0). **(A and B)** Two-chamber view in diastole/systole. **(C and D)** Short-axis view in diastole/systole. Abbreviation as in Figure 1.

COMPARISON OF THE NEW SINGLE-BREATH-HOLD CS APPROACH VERSUS THE STANDARD MULTI-BREATH-HOLD CINE MR TECHNIQUE. The conventional cine MR acquisitions were used as the "gold standard" for measurements of LVEF, left ventricular end-diastolic volume (LVEDV), left ventricular end-systolic volume (LVESV), LVSV, and LV mass. These images were collected with 4 to 6 breath-holds, yielding 8 to 12 short-axis slices (the 3 long-axis acquisitions were used occasionally to decide on the most basal short-axis slice to be included for analysis; otherwise, the long-axis acquisitions were not used for analysis). For the acquisition of the CS cine data, 2 breath-holds were performed (1 non-cine acquisition to check for fold-over and 1 cine acquisition). The CS cine acquisitions yielded a similar LVEF of 48.5 ± 15.9% versus 49.8 ± 15.8% measured by the standard multi-breath-hold technique (p = 0.11). Excellent agreement was obtained by Bland-Altman analysis (Figure 6).

LVEDV was slightly smaller by 6.0 ± 10.2% (p = 0.0009) when measured by the CS approach, whereas no differences were found for LVESV, LVSV, and LV mass (Table 4). Bland-Altman and linear regression analyses yielded good agreement for all 4 parameters (Figure 7).

VALIDATION OF THE NEW SINGLE-BREATH-HOLD MULTISLICE CS APPROACH. In the group of 12 healthy volunteers, excellent correlation was found between $LVSV_{CS}$ and aortic flow, with an overestimation by $LVSV_{CS}$ of 5.6 ± 6.5 ml/beat as illustrated in Figure 8A. The standard multi-breath-hold CMR approach overestimated by 16.2 ± 11.7 ml/beat (p = 0.012 vs. CS) (Table 4, Figure 8C), and its variability versus the reference aortic flow was larger (Figures 8B and 8D).

INTRAOBSERVER AND INTEROBSERVER VARIABILITY OF THE NEW SINGLE-BREATH-HOLD CS APPROACH. Intraobserver and interobserver variabilities for the

new CS approach were excellent, as given in Table 5. The intraobserver and interobserver differences ranged from −3.8% to −0.4% and from −9.7% to +0.7%, respectively, with slopes of regressions ranging between 0.94 and 1.06 and between 0.93 and 1.06, respectively (Table 5).

DISCUSSION

PERFORMANCE OF THE SINGLE-BREATH-HOLD CS APPROACH AND COMPARISON WITH OTHER TECHNIQUES. Overall, the single-breath-hold CS approach yielded a high image quality in 94% of all participants (Table 3), and all examinations were of sufficient quality to undergo quantitative 3D LV model-based analysis. With recently-established quality criteria applied (9), a score ≥3 (i.e., artifacts in ≥3 slices) was obtained in only 2 participants (6% of study participants). The standard cine CMR technique is known to yield good image quality in patients equipped with MR-conditional pacemakers (21), and similarly, an excellent quality was achieved with the CS approach in a pacemaker-implanted patient as illustrated in Figure 4. The high image quality of the CS technique translated into high agreement for LVEF, with a mean difference versus the standard multi-breath-hold technique of 1.3% (95% confidence interval [CI]: −7.2% to +9.7%). For interstudy variabilities of the standard LVEF measurements, 95% CIs of −4.1% to +4.3% were reported (22,23), which are only slightly narrower than the differences found between the standard cine and CS technique in the current study. Thus, the variability between the standard and CS technique observed in the current study was comparable to the reproducibility of the standard technique itself. Accordingly, the novel CS-based technique, although much faster than the standard approach, may be reproducible and accurate enough to replace the standard multi-breath-hold CMR approach.

High agreement between the standard and CS technique was also achieved for LVESV, with a nonsignificant difference of 2.0 ml (Table 4). With the presented single-breath-hold CS technique, LV mass was also measured accurately, with a difference versus the standard technique of 2% (95% CI: −16.8% to +12.8%). This interval for LV mass quantification is small considering that the intraoperator variability for standard multi-breath-hold LV mass measurements was reported to be −12.3% to +15.9% (22).

However, LVEDV was statistically smaller with the CS approach by 9.9 ml (Table 4). Similarly, with other highly-accelerated single-breath-hold techniques that are based on spatiotemporal correlations

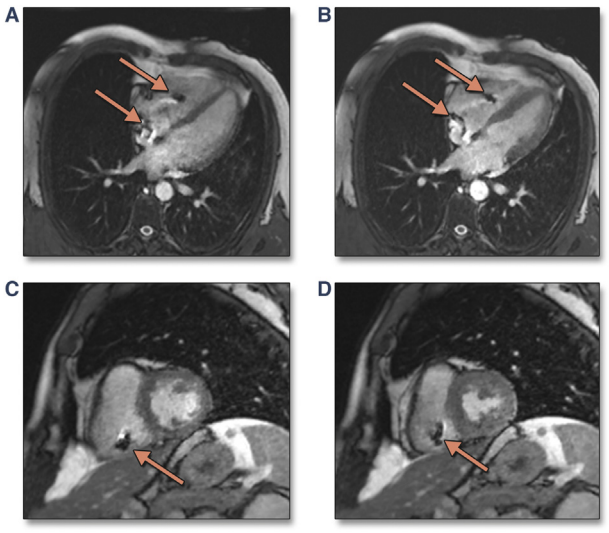

FIGURE 4 Good-Quality Compressed Sensing Acquisition in a 56-Year-Old Patient

Patient had a dual-chamber pacemaker **(arrows)** (Advisa MRI SureScan System, Medtronic Inc., Mounds View, Minnesota) implanted for complete atrioventricular block of unknown origin. Cardiac magnetic resonance imaging was requested for the detection of myocarditis or infiltrative cardiomyopathy. The pacemaker leads are visible in the right atrium and right ventricle **(arrows)** without affecting the image quality (quality score of 0 [good]). **(A and B)** Four-chamber view in diastole/systole. **(C and D)** Short-axis view in diastole/systole.

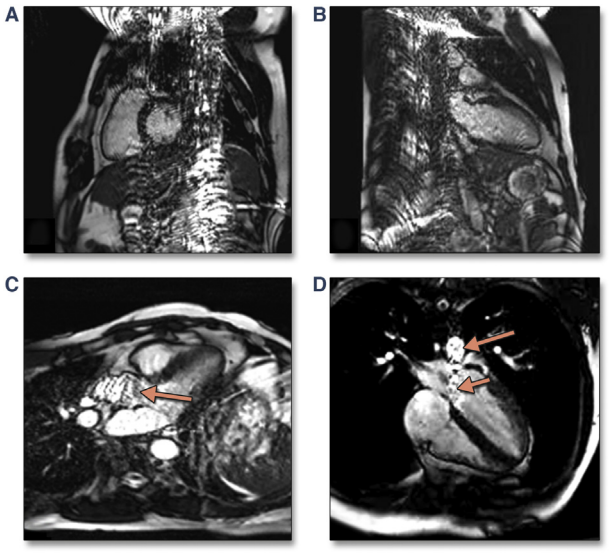

FIGURE 5 Fold-Over Artifact in the Superior-Inferior Direction on Short-Axis and 2-Chamber Views

(A) Short-axis view. **(B)** Two-chamber view. Quality score is 3 (fold-over artifacts in >3 slices). Flow-related artifacts in phase-encoding direction **(arrows)** on systolic phases in a volunteer propagating over the aortic valve in the 3-chamber view **(C)** and over the mitral valve in the 4-chamber view **(D)**. Quality score is 1 (image blurring in 1 slice, apical region in **C**).

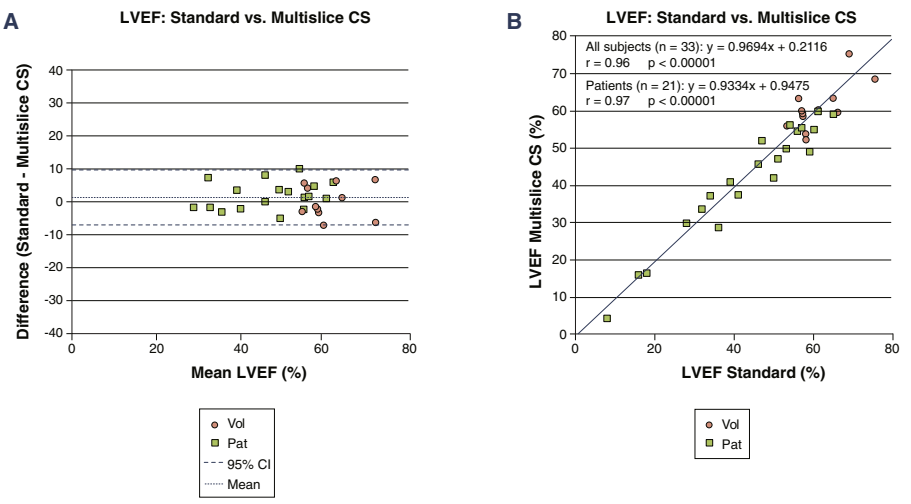

FIGURE 6 LVEF Quantification of CS and Standard Cardiac Magnetic Resonance

(A) Bland-Altman. **(B)** Linear regressions (**diagonal line** is line of identity). CI = confidence interval; CS = compressed sensing; LVEF = left ventricular ejection fraction; Pat = patient; Vol = volunteer.

such as kt-BLAST (12), TPAT (13), or TSENSE (24), slightly smaller LVEDVs (−8.2 to −4.9 ml) and slightly larger LV mass (1.1 to 13.1 g) were found versus the conventional multi-breath-hold technique (LVESV was not significantly different). Temporal filtering of the accelerated acquisitions could result in such an underestimation of LVEDV if, for example, the increase in LV volume during atrial contraction was missed. In preliminary tests, we determined the CS parameters that could track the premature septal contraction in left bundle branch block, a short-lived contraction occurring during the first 30 to 60 ms after the R-wave trigger (25). Thus, the presented technique is able to detect phenomena occurring immediately after the R-wave. Alternatively, at a lower signal-to-noise ratio, the endocardial border, and consequently blood-filled intertrabecular spaces, might be less well detected, potentially resulting in a "smaller" endocardial contour (i.e., underestimation of LVEDV and overestimation of LV mass). If blood-filled intertrabecular spaces are nearly absent in the "compacted" end-systolic phase and are "underestimated" in end-diastole by accelerated techniques, this may result in more precise ejection volumes, which was observed in this study because $LVSV_{CS}$ correlated better with aortic flow than the standard approach.

TABLE 4 Comparison of Standard Multi-Breath-Hold CMR Versus Single-Breath-Hold Multislice CS Technique and Validation

	Standard CMR (n = 33)	CS Technique CMR (n = 33)	Mean Difference	p Value
LVEF, %	49.8 ± 15.8	48.5 ± 15.9	1.3 ± 4.3	0.11
LVEDV, ml	176.4 ± 56.9	166.5 ± 59.0	9.9 ± 10.2	0.0009
LVESV, ml	94.5 ± 63.2	92.4 ± 66.4	2.0 ± 11.7	0.24
LVSV, ml	82.8 ± 25.6	74.1 ± 22.7	8.7 ± 12.8	0.11
LV mass, g	128.8 ± 32.1	131.2 ± 32.6	−2.5 ± 9.6	0.18
Validation (n = 12 volunteers)				
	Aortic flow reference	CS technique CMR		
Flow – LVSV, ml	86.3 ± 16.1	91.9 ± 14.1	−5.6 ± 6.5	0.01
	Aortic flow reference	Standard CMR		
Flow – LVSV, ml	86.3 ± 16.1	102.4 ± 15.3	−16.2 ± 11.7	0.0006

Values are mean ± SD.
Abbreviations as in Tables 1 and 2.

The presented CS approach acquires 1 slice per 2 heart beats, whereas kt-BLAST acquires 1 slice per 1.6 heart beats (12) and TPAT acquires 1 slice per 2.5 heart beats (13). If the acquisition time is corrected for spatial resolution, the CS approach is approximately 2 and 3 times faster than kt-BLAST and TPAT, respectively, and it is 4 to 5 times faster than TPAT if corrected for temporal resolution. The elegant real-time CS approach of Feng et al. (26) acquires 1 slice per heart beat, but voxels are 3 times larger and temporal resolution is 1.5 times lower versus that in the current

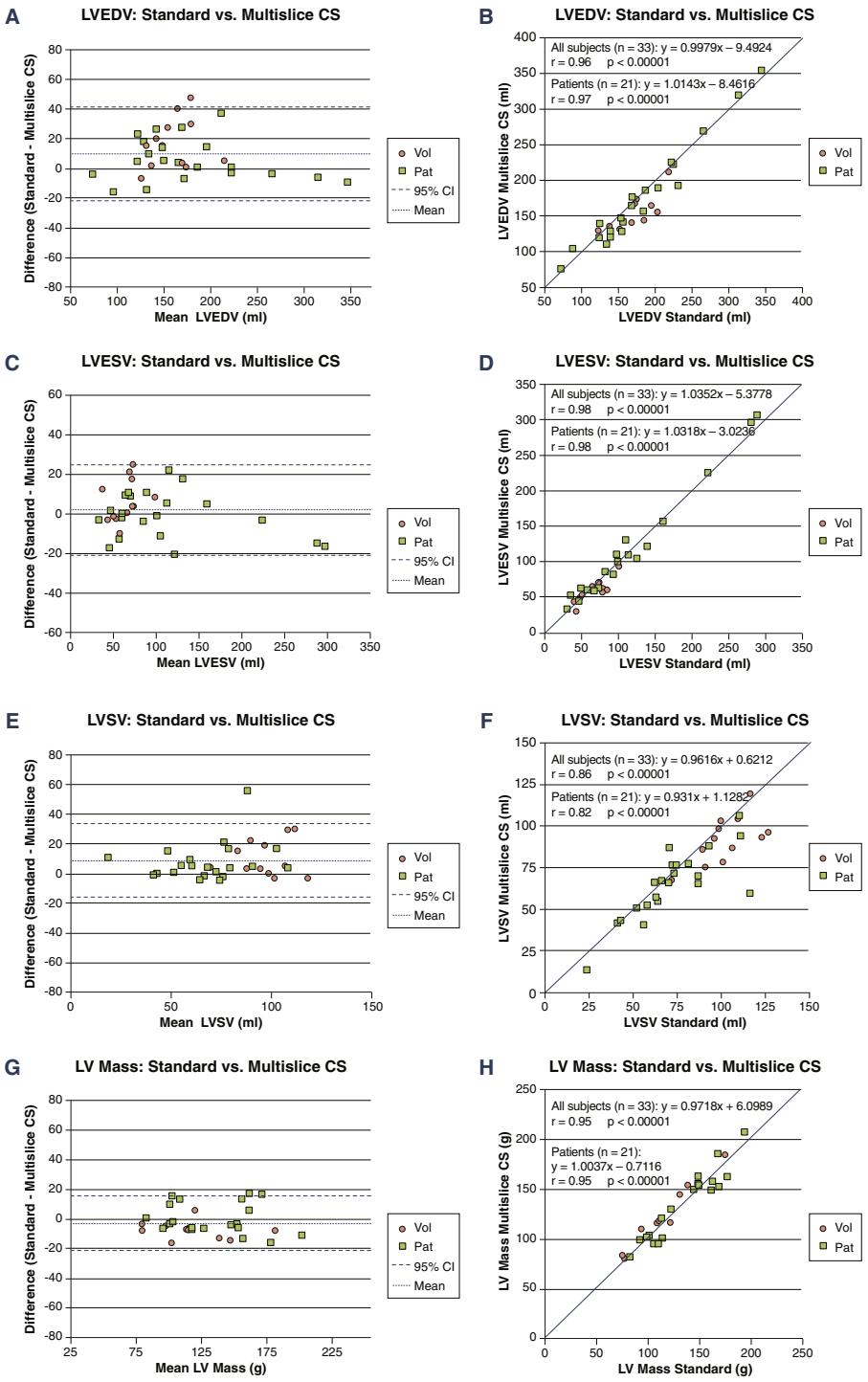

FIGURE 7 Quantification of LVEDV, LVESV, LVSV, and LV Mass of CS and Standard Cardiac Magnetic Resonance

(A, C, E, and G) Bland-Altman. **(B, D, F, and H)** Linear regressions (**diagonal line** is line of identity). LVEDV = left ventricular end-diastolic volume; LVESV = left ventricular end-systolic volume; LVSV = left ventricular stroke volume; other abbreviations as in Figure 6.

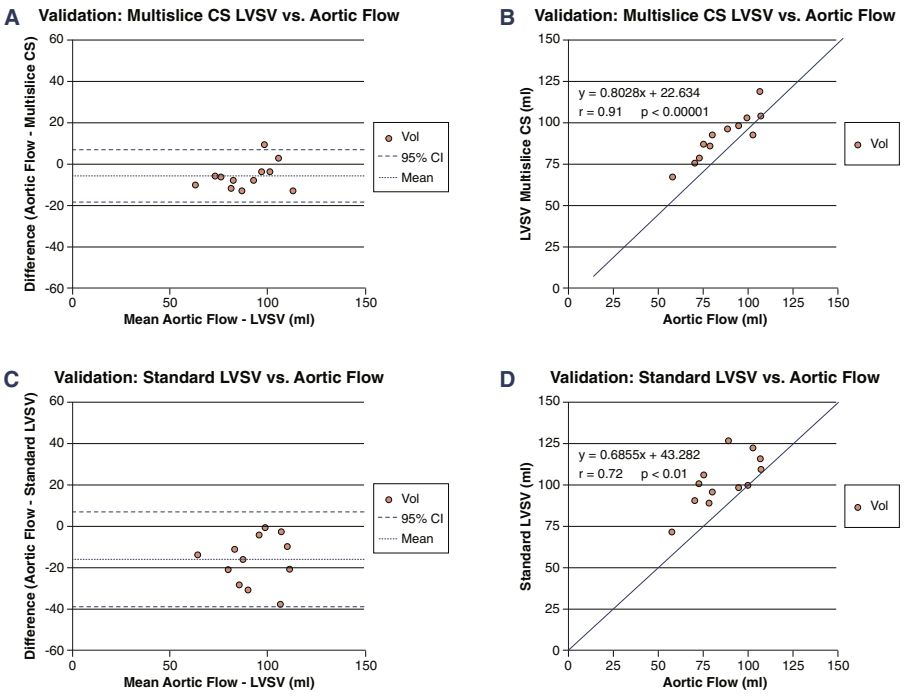

FIGURE 8 Validation of CS and Standard Cardiac Magnetic Resonance Imaging for Quantification of LVSV Versus Aortic Outflow

(A and C) Bland-Altman. **(B and D)** Linear regressions (**diagonal line** is line of identity). The novel CS approach was more accurate than the conventional technique (**A and C:** underestimation of 5.6 ± 6.5 ml vs. 16.2 ± 11.7 ml; p = 0.012), and its variability versus aortic flow was lower **(B and D)**. Abbreviations as in Figures 6 and 7.

study. Future studies are needed to determine whether this higher speed achieved by the presented CS approach is translated into higher accuracy and reproducibility versus other highly-accelerated techniques.

The presented CS technique also offers the advantage that functional information in at least a single plane can be obtained in patients unable to hold their breath for several heart beats or in patients with arrhythmias.

VALIDATION OF THE NOVEL SINGLE-BREATH-HOLD CS TECHNIQUE. To accurately account for the long-axis shortening of the LV, a set of radial long-axis acquisitions was proposed, which achieved good reproducibility in humans and excellent agreement for volumes in porcine hearts (27). In the current approach, we combined long-axis CS acquisitions to benefit from their high in-plane spatial resolution to accurately assess the position of the mitral valve annulus, and short-axis CS acquisitions were added to minimize partial volume artifacts that can occur near the papillary muscles on long-axis orientations. In the volunteer group without mitral insufficiency, the flow in the ascending aorta was used as a reference for LVSV. When this multislice CS acquisition scheme was combined with the 3D LV model-based analysis, the LVSV results indicated that the single-breath-hold CS approach was more accurate than the conventional multi-breath-hold approach when volumetric LVSV was compared with aortic flow (difference 5.6 ml vs. 16.2 ml, respectively; p = 0.012) (Figure 8A). More importantly, $LVSV_{CS}$ was not only more precise but also less variable than that found with the conventional approach (i.e., smaller SD of 6.5 ml/beat vs. 11.7 ml/beat of the standard multi-breath-hold approach in comparison with aortic flow) (Table 4, Figure 8B). One might infer from these LVSV results that LVEDV and LVESV were also measured more accurately by the CS approach as compared with the conventional multi-breath-hold approach. Most likely the higher accuracy of the CS approach was due to the fact that this technique allows correct tracking of the 3D motion of the base of the heart during the cardiac cycle;

inaccurate slice positioning at the base of the heart with conventional short-axis slices can translate into relatively large errors (28). Furthermore, with a single-breath-hold approach, all acquired slices are registered in space, which allows for more precise post-processing. With an accurate measurement of the LVSV, the quantification of mitral insufficiency should theoretically benefit (when mitral regurgitant volume is calculated as LVSV − aortic forward flow).

We observed a slight overestimation of the $LVSV_{CS}$ of 5.6 ml/beat in comparison with that of aortic flow. Because underestimation of aortic flow by the phase-contrast technique is unlikely in tricuspid aortic valves (29), overestimation of $LVSV_{CS}$ may be considered. LV trabeculations are typically included into the endocardial LV contour in the end-diastolic but less so in the compacted end-systolic phase, potentially resulting in a small underestimation of LVESV and thus overestimation of LVSV. Captur et al. (30) reported a mass of LV trabeculations in volunteers of 8.2% of the total LV mass (corresponding to 10.1 g in our volunteer population), which can explain the small overestimation of the LVSVCS in the present study.

ROBUSTNESS OF THE NEW SINGLE-BREATH-HOLD MULTISLICE CS APPROACH. For the LVEF measurements by the CS technique, intraobserver and interobserver reproducibilities were ±3.4% and ±3.9%, respectively (see **Table 5** for SD of the differences). For the interobserver variability of the standard multi-breath-hold technique, ±3% to ±6% were reported (31,32), closely matching the reproducibility of the novel CS technique. Similarly, for the LVESV, the reported SD was approximately ±9.5% in volunteers (32) and ±7 ml in patients (31), again matching the ±8.4% and ±7.5 ml for the CS technique.

However, for LVEDV and LV mass, SDs of approximately ±1% and ±5.5% (32) and ±5.5 ml and ±6.5 g (31) were achieved, respectively, which are lower than the CS values reported here (±8.4%, ±9.6%, ±11.2 ml, and ±13.7 g, respectively).

STUDY LIMITATIONS. It should be mentioned that this accelerated single-breath-hold CS approach is adequate for LVEF and LV volume/mass measurements, whereas the evaluation of small pathological structures as present in cardiomyopathies or congenital heart diseases is assumed to be more reliable when performed on conventional cine images.

A current limitation of the CS approach is its susceptibility for fold-over artifacts (**Figures 5A and 5B**). Therefore, the field of view must cover the entire anatomy, and thus, some penalty in spatial resolution may occur in relation to the patient's anatomy. In addition, the sparsity in the temporal domain may be limited in anatomic regions of very high flow; therefore, in some acquisitions, flow-related artifacts occurred in the phase-encoding direction during systole (**Figures 5C and 5D**). Also, in its current version, the sequence was prospectively triggered; thus, it did not cover the very last phases of the cardiac cycle. Finally, the reconstruction times for the CS images lasted 1.75 min, precluding an immediate assessment of image quality or using these images to plan next steps of a CMR examination. However, graphic processing unit-based reconstruction algorithms can be used in the future to overcome this limitation.

TABLE 5 Intraobserver and Interobserver Variabilities of the Single-Breath-Hold Multislice CS Technique

	Bland-Altman (n = 33)				Correlation (n = 33)		
	Mean	SD	% Mean	% SD	r	slope	p Value
Intraobserver							
LVEF, %	−0.4	±3.4	−2.5	±13.3	0.97	0.99	<0.00001
LVEDV, ml	−2.1	±6.5	−1.4	±4.5	0.99	0.99	<0.00001
LVESV, ml	0.1	±4.5	−0.4	±7.0	0.99	1.02	<0.00001
LVSV, ml	−2.2	±8.1	−3.8	±15.0	0.94	0.94	<0.00001
LV mass, g	−0.5	±11.2	−0.8	±7.9	0.93	1.06	<0.00001
Interobserver							
LVEF, %	1.1	±3.9	0.7	±19.0	0.96	1.02	<0.00001
LVEDV, ml	−10.8	±11.2	−7.4	±8.4	0.98	1.06	<0.00001
LVESV, ml	−7.0	±7.5	−9.7	±11.0	0.99	1.03	<0.00001
LVSV, ml	−3.8	±10.0	−6.6	±21.4	0.90	1.03	<0.00001
LV mass, g	0.1	±13.7	−0.2	±9.6	0.92	0.93	<0.00001

Abbreviations as in **Tables 1 and 2**.

CONCLUSIONS

The results showed that CS-based MR acquisitions were applicable to the heart in a clinical setting. This novel, fast acquisition strategy allows for covering the entire LV with high temporal and spatial resolution within a single breath-hold. The image quality based on these results is adequate to yield highly accurate measures of LVEF, LV volumes, and LV mass.

REPRINT REQUESTS AND CORRESPONDENCE: Dr. Juerg Schwitter, Division of Cardiology and Director Cardiac MR Center, University Hospital of Lausanne, Rue du Bugnon 46, 1011 Lausanne, Switzerland. E-mail: jurg.schwitter@chuv.ch.

REFERENCES

1. Curtis JP, Sokol SI, Wang Y, et al. The association of left ventricular ejection fraction, mortality, and cause of death in stable outpatients with heart failure. J Am Coll Cardiol 2003;42:736–42.

2. Gharib MI, Burnett AK. Chemotherapy-induced cardiotoxicity: current practice and prospects of prophylaxis. Eur J Heart Fail 2002;4:235–42.

3. Bardy GH, Lee KL, Mark DB, et al. Amiodarone or an implantable cardioverter-defibrillator for congestive heart failure. N Engl J Med 2005;352:225–37.

4. Sürder D, Manka R, Lo Cicero V, et al. Intracoronary injection of bone marrow-derived mononuclear cells early or late after acute myocardial infarction: effects on global left ventricular function. Circulation 2013;127:1968–79.

5. Hunt SA, Abraham WT, Chin MH, et al. 2009 focused update incorporated into the ACC/AHA 2005 Guidelines for the Diagnosis and Management of Heart Failure in Adults. J Am Coll Cardiol 2009;53:e1–90.

6. McMurray JJV, Adamopoulos S, Anker SD, et al. ESC guidelines for the diagnosis and treatment of acute and chronic heart failure 2012. Eur Heart J 2012;33:1787–847.

7. Kramer C, Barkhausen J, Flamm S, et al. Standardized cardiovascular magnetic resonance (CMR) protocols 2013 update. J Cardiovasc Magn Reson 2013;15:91.

8. Kilner PJ, Geva T, Kaemmerer H, et al. Recommendations for cardiovascular magnetic resonance in adults with congenital heart disease from the respective working groups of the European Society of Cardiology. Eur Heart J 2010;31:794–805.

9. Klinke V, Muzzarelli S, Lauriers N, et al. Quality assessment of cardiovascular magnetic resonance in the setting of the European CMR Registry: description and validation of standardized criteria. J Cardiovasc Magn Reson 2013;15:55.

10. Bruder O, Wagner A, Lombardi M, et al. European Cardiovascular Magnetic Resonance (EuroCMR) Registry—multi national results from 57 centers in 15 countries. J Cardiovasc Magn Reson 2013;15:1–9.

11. Kozerke S, Plein S. Accelerated CMR using zonal, parallel and prior knowledge driven imaging methods. J Cardiovasc Magn Reson 2008;10:29.

12. Jahnke C, Nagel E, Gebker R, et al. Four-dimensional single breathhold magnetic resonance imaging using kt-BLAST enables reliable assessment of left- and right-ventricular volumes and mass. J Magn Reson Imaging 2007;25:737–42.

13. Eberle H, Nassenstein K, Jensen C, et al. Rapid MR assessment of left ventricular systolic function after acute myocardial infarction using single breath-hold cine imaging with the temporal parallel acquisition technique (TPAT) and 4D guide-point modelling analysis of left ventricular function. Eur Radiol 2010;20:73–80.

14. Plein S, Schwitter J, Suerder D, et al. k-t SENSE-accelerated myocardial perfusion MR imaging at 3.0 Tesla—comparison with 1.5 Tesla. Radiology 2008;249:493–500.

15. Schwitter J, Oelhafen M, Wyss BM, et al. 2D-spatially-selective real-time magnetic resonance imaging for the assessment of microvascular function and its relation to the cardiovascular risk profile. J Cardiovasc Magn Reson 2006;8:759–69.

16. Lustig M, Donoho D, Pauly JM. Sparse MRI: the application of compressed sensing for rapid MR imaging. Magn Reson Med 2007;58:1182–95.

17. Liu J. Dynamic cardiac MRI reconstruction with weighted redundant Haar wavelets (abstr). Proc Int Soc Magn Reson Med 2012;67:4249.

18. Young AA, Cowan BR, Thrupp SF, Hedley WJ, Dell'Italia LJ. Left ventricular mass and volume: fast calculation with guide-point modeling on MR images. Radiology 2000;216:597–602.

19. Schwitter J, DeMarco T, Kneifel S, et al. Magnetic resonance-based assessment of global coronary flow and flow reserve and its relation to left ventricular functional parameters: a comparison with positron emission tomography. Circulation 2000;101:2696–702.

20. Bland J, Altman D. Statistical methods for assessing agreement between two methods of clinical measurement. Lancet 1986;1:307–10.

21. Schwitter J, Kanal E, Schmitt M, et al. Impact of the Advisa MRI pacing system on the diagnostic quality of cardiac MR images and contraction patterns of cardiac muscle during scans: Advisa MRI randomized clinical multicenter study results. Heart Rhythm 2013;10:864–72.

22. Danilouchkine M, Westenberg J, De Roos A, Reiber J, Lelieveldt P. Operator induced variability in cardiovascular MR: left ventricular measurements and their reproducibility. J Cardiovasc Magn Reson 2005;7:447–57.

23. Grothues F, Smith G, Moon J, et al. Comparison of interstudy reproducibility of cardiovascular magnetic resonance with 2-dimensional echocardiography in normal subjects and in patients with heart failure or left ventricular hypertrophy. Am J Cardiol 2002;90:29–34.

24. Young A, Cowan B, Schoenberg S, Wintersperger B. Feasibility of single breath-hold left ventricular function with 3 Tesla TSENSE acquisition and 3D modeling analysis. J Cardiovasc Magn Reson 2008;10:24.

25. Rutz AK, Manka R, Kozerke S, et al. Left ventricular dyssynchrony in patients with left bundle branch block and patients after myocardial infarction: integration of mechanics and viability by cardiac magnetic resonance. Eur Heart J 2009;30:2117–27.

26. Feng L, Srichai MB, Lim RP, et al. Highly accelerated real-time cardiac cine MRI using k-t SPARSE-SENSE. Magn Reson Med 2013;70:64–74.

27. Bloomer T, Plein S, Radjenovic A, et al. Cine MRI using steady-state free precession in the radial long-axis orientation is a fast accurate method for obtaining volumetric data of the left ventricle. J Magn Reson Imaging 2001;14:685–92.

28. Marcus J, Goette M, DeWaal L, et al. The influence of through-plane motion on left ventricular volumes measured by magnetic resonance imaging: implications for image acquisition and analysis. J Cardiovasc Magn Reson 1999;1:1–6.

29. Muzzarelli S, Monney P, O'Brien K, et al. Quantification of aortic flow by phase-contrast magnetic resonance in patients with bicuspid aortic valve. Eur Heart J Cardiovasc Imaging 2013;15:77–84.

30. Captur G, Muthurangu V, Cook C, et al. Quantification of left ventricular trabeculae using fractal analysis. J Cardiovasc Magn Reson 2013;15:36.

31. Papavassiliu T, Kühl HP, Schröder M, et al. Effect of endocardial trabeculae on left ventricular measurements and measurement reproducibility at cardiovascular MR imaging. Radiology 2005;236:57–64.

32. Moon J, Lorenz C, Francis J, Smith G, Pennell D. Breath-hold FLASH and FISP cardiovascular MR imaging: left ventricular volume differences and reproducibility. Radiology 2002;223:789–97.

KEY WORDS cardiac function, fast imaging, fast LV assessment

APPENDIX For supplemental information, please see the online version of this article.